Clim. Past Discuss., 11, 1913–1943, 2015
www.clim-past-discuss.net/11/1913/2015/
doi:10.5194/cpd-11-1913-2015

Climate of the Past
Discussions
Open Access

Miocene–Pliocene stepwise intensification of the Benguela upwelling over the Walvis Ridge off Namibia

S. Hoetzel[1], L. M. Dupont[1], F. Marret[2], G. Jung[1], and G. Wefer[1]

[1]MARUM – Center for Marine Environmental Sciences, University of Bremen, Leobenerstr., Bremen, Germany
[2]School of Environmental Sciences, University of Liverpool, L69 7ZT, UK

Received: 8 April 2015 – Accepted: 30 April 2015 – Published: 20 May 2015

Correspondence to: L. M. Dupont (ldupont@marum.de)

Published by Copernicus Publications on behalf of the European Geosciences Union.

Abstract

Upwelling is a significant part of the ocean circulation controlling largely the transport of cold waters to the surface and therefore influences ocean productivity and global climate. The Benguela Upwelling System (BUS) is one of the major upwelling areas in the world. Previous reconstructions of the BUS mainly focused on the onset and intensification in southern and central parts, but changes of the northern part have been rarely investigated in detail. Using the organic-walled dinoflagellate cyst record of ODP Site 1081 from the Late Miocene to the Pliocene we reconstruct and discuss the upwelling history on the Walvis Ridge with a special focus on the movement of the Angola–Benguela Front (ABF). We show that during the Late Miocene the Angola Current flowed southwards over the Walvis Ridge more frequently than today because the ABF was probably located further south as a result of a weaker meridional temperature gradient. A possible strengthening of the meridional gradient during the latest Miocene to early Pliocene in combination with uplift of south-western Africa intensified the upwelling along the coast and increased the upwelling's filaments over the Walvis Ridge. An intermediate period from 6.2 to 5.5 Ma is shown by the dominance of *Habibacysta tectata*, cysts of a cool-tolerant dinoflagellate known from the northern Atlantic, indicating changing oceanic conditions contemporaneous with the Messinian Salinity Crisis. From 4.4 Ma on, the upwelling signal got stronger again and waters were well-mixed and nutrient-rich. Also effects of Cunene River discharge into the South Atlantic are recorded since 4.4 Ma. Our results show a northward migration of the ABF and the initial stepwise intensification of the BUS.

1 Introduction

The south-western coast of Africa is currently characterised by cold and nutrient-rich waters related to the occurrence of the Benguela Upwelling System (BUS), favouring high primary production. It is one of the major upwelling areas in the world. This system

CPD
11, 1913–1943, 2015

is supposed to have initiated in the early Late Miocene (~ 10–15 Ma) (Siesser, 1980; Diester-Haass et al., 1990; Heinrich et al., 2011; Rommerskirchen et al., 2011) during a phase of global cooling. This cooling is part of the transition from a warm and humid variable climate to cooler and drier conditions of the late Neogene driven by changes of the Antarctic ice sheets (Wright et al., 1992; Zachos et al., 2001; Billups and Schrag, 2002). Later, the BUS probably played a decisive role in the climate development of the latest Neogene (Etourneau et al., 2012).

Following the mid Miocene climatic optimum, the re-establishment of major ice sheets in East Antarctica at around 10 Ma led to a globally steeper meridional temperature gradient which would have intensified pressure systems and ocean circulations (Flower and Kennett, 1994; Zachos et al., 2001); the South Atlantic Anticyclone (SAA) became stronger and with it the SE trade winds which led to increased upwelling and marine productivity especially at around 6.5 Ma (Diester-Haass et al., 2002). These authors hypothesized that the further growth of the Antarctic ice sheets led to a northward migration of the Antarctic Polar Front causing also a shift of the BUS and changing the composition of the water (Diester-Haass, 1988; Diester-Haass et al., 1990, 1992). However, recent modelling showed that the introduction of an ice-cap in Antarctica resulted in strong downwelling in the Weddell Sea which attracted warmer water from lower latitudes effectively reducing the meridional sea-surface temperature (SST) gradient in the Atlantic sector of the Southern Ocean. This resulted for the BUS region in slightly reduced Ekman pumping, less upwelling, and warmer subsurface temperatures (Goldner et al., 2013; Knorr and Lohmann, 2014; Jung et al., 2014). On the other hand, the ongoing uplift of Southern Africa during the late Miocene and Pliocene (Partridge, 1997; Roberts and White, 2010) would have strengthened the low-level winds along the southwest African coast (Benguela Jet) enhancing upwelling in the BUS, especially in the central part. A comparison of different model experiments estimates the effects of uplift of Southern Africa on the surface winds driving the BUS far greater than the effects of far field tectonic changes such as the closure of the Central American Seaway (CAS) or the narrowing of the Indonesian Seaway. However, a subsurface cooling

CPD
11, 1913–1943, 2015

increasing with depth was found in the case of CAS closure, which indicates the possibility of changing ocean surface conditions in the Benguela region even if upwelling remained constant (Jung et al., 2014).

More important to the conditions in the BUS would be the effect of the CAS closure on the deep water formation in the Atlantic. According to Billups (2002), the closure of the CAS had already influenced the ocean currents between 6.6 and 6 Ma by increasing the Atlantic overturning circulation (AMOC). The data sets show a cooling of Southern Ocean upper circumpolar and intermediate waters during the latest Miocene. Poore et al. (2006) calculated the proportion of North Atlantic Deepwater (Northern Component Water) and describe an increase of Northern Component Water formation as well as a stronger AMOC for the period between 6 and 2 Ma. The influence of the closing of the CAS on the AMOC is furthermore underlined by models such as the one used by Butzin et al. (2011) who concluded that the formation of North Atlantic Deepwater (NADW) began when the CAS had shoaled to a few hundred meters during the Late Miocene.

A number of paleostudies focused on the upwelling history of either in the southern and central parts of the BUS or on the ocean side of the Walvis Ridge (Siesser, 1980; Diester-Haass et al., 1992; Marlow et al., 2000; Berger et al., 2002b; Udeze and Obohikuenobe, 2005; Heinrich et al., 2011; Rommerskirchen et al., 2011; Rosell-Melé et al., 2014), whereby only ODP Site 1085 in the southern BUS covers its history since the late Miocene (past 14 Ma). ODP Site 1084 in the central BUS area only covers the Pliocene down to ~ 5 Ma. ODP Site 1081, which sediments cover the past 9 Ma, sits at the northern end of the modern BUS. Therefore, the site is sensitive to changes at the northern boundary and to movements of the Angola–Benguela Front (ABF). Furthermore, the site is located on the Walvis Ridge (Wefer et al., 1998) which divides the Cape Basin and the Benguela Current from the Angola Basin and the warm waters of the Angola Current. We use a multi-proxy approach to constrain changes in sea-surface conditions between the late Miocene and Pliocene (9 to 2.7 Ma), with assemblages of organic-walled dinoflagellate cysts as primary proxies, and more particularly

CPD
11, 1913–1943, 2015

to describe changes on the northern edge of the BUS during times of global cooling as well as discuss forcing mechanisms. We complement our results on dinoflagellate cysts with total organic carbon measurements (new and shipboard data) and compare them with alkenone-derived SSTs (Hoetzel et al., 2013). Studies on recent distribution of dinoflagellate cysts along the West African coast (e.g. Dale et al., 2002; Marret and Zonneveld, 2003; Zonneveld et al., 2013) enable us to associate the oceanographic context (upwelling vs. oligotrophic conditions) with specific cyst assemblages.

2 The modern Benguela Upwelling System

The semi-permanent high pressure system, the SAA, over the South East Atlantic is the dominating atmospheric feature located at around 32° S 5° W (austral summer) and 27° S 10° W (austral winter) (Petterson and Stramma, 1991) (Fig. 1). The SAA is driving the Benguela Current (BC) which flows northwards along the south-western coast of Africa. The BC contains water from the eastward flowing cold Antarctic Circumpolar Current (ACC), which is linked to the polar front. It also takes up water from the warm Agulhas Current (AgC), which is flowing from the Indian Ocean around South Africa. At around 28° S the BC divides into two separate currents; one following the rotation of the SAA turning west crossing the Atlantic and the other flowing further northwards along the south-western African coast under the name of Benguela Coastal Current (BCC). Additionally, the BCC is linked to the south-easterly trade winds (Petterson and Stramma, 1991).

The coastal-parallel winds push the coastal surface waters via Ekman-transport off shore inducing the upwelling of cold and nutrient-rich subsurface waters (e.g. Lutjeharms and Meeuwis, 1987). The upwelled nutrients allow a vast production of phytoplankton in the photic zone. Eight upwelling cells have been identified, of which the one west of Lüderitz Bay is the strongest persisting all year long resulting in the coldest surface waters of the BUS (Lutjeharms and Meeuwis, 1987). Up to 600 km off shore cold upwelled waters from the coastal upwelling areas mix with surface waters and form nutrient-rich filaments (Lutjeharms and Meeuwis, 1987; Lutjeharms and Stockton, 1987; Summerhayes et al., 1995). Water of these filaments has clearly enhanced nutrient values, lower temperatures and increased primary production.

The BCC meets the southward-flowing warm and nutrient-poor Angola Current just north of the Walvis Ridge. Together they form the ABF which today is situated between 14 and 16° S (Meeuwis and Lutjeharms, 1990), dependent on the season. In detail, it is not a single front but a couple of fronts arranged in two frontal zones, a northern and a southern one, whereas the latter one has the larger influence on the overall ABF's characteristics (Kostianoy and Lutjeharms, 1999). Like the coastal upwelling, the position of the front depends on the SAA; when the meridional pressure gradient is high, the southern front of the ABF is located further north and the ABF is narrower and sharper (Kostianoy and Lutjeharms, 1999). Under weakened SAA conditions and resulting weakened winds, the ABF can be located further to the south (Richter et al., 2010) so that warm nutrient-poor water of the Angola current can penetrate further southward as far as 24° S along the Namibian coast (Meeuwis and Lutjeharms, 1990). As a result, the precipitation on the adjacent coast is enhanced (Hirst and Hastenrath, 1983; Nicholson and Entekhabi, 1987) and can be increased farther inland (Rouault, 2003). The phenomenon occurs on inter-annual timescales and is called Benguela Niño for its similarity to the El Niño Southern Oscillation (Shannon et al., 1986).

3 The material and methods

The sampled sediment core was retrieved at the Ocean Drilling Program Site 1081 (19°37′ S 11°19′ E) in 794 m water depth. The site is located on the Walvis Ridge 160 km off the Namibian coast and is today influenced by filaments of the BUS. The sediment is composed of olive-gray clayey nannofossil ooze and olive-gray to black clays (Wefer et al., 1998). Sedimentation rates were calculated between 2 and 5 cm ka^{-1} using an age model based on biostratigraphy, magnetic reversals and magnetic susceptibility (Berger et al., 2002b).

CPD
11, 1913–1943, 2015

Seventy-one samples were taken with ages between 9 and 2.7 Ma and prepared for palynological investigation. The volume of each sample was estimated by water displacement. For decalcification diluted cold HCl (~ 5%) was used and afterwards the material was set in cold HF (~ 20%) for two days to remove silicates. Prior to the HCl-treatment *Lycopodium* tablets were added. The residuals were sieved under ultrasonic treatment removing particles smaller than 10–15 µm. The cleaned residues were stored in water and mounted in glycerol for investigation under a light microscope using magnifications of 400×, 600× and 1000×. For each sample at least 300 dinoflagellate cysts were identified and counted.

Identification of dinoflagellate cysts was done after De Verteuil and Norris (1992), Marret and Zonneveld (2003), De Schepper and Head (2009) and Schreck et al. (2012). *Brigantedinium* spp. includes all round brown smooth dinoflagellate cysts. Because *Batiacasphaera micropapillata* has a strong morphological overlap with *B. minuta* and both occur in the samples we adopted the nomenclature of De Schepper and Head (2008) and Schreck et al. (2012) in treating both species as one complex.

Each species was ecologically sorted after its assumed metabolism mechanism (autotroph and heterotroph, Table 1) and a heterotroph/autotroph ratio (H/A) was calculated expressed as ln(H/A). Percentages were calculated on the total number of dinoflagellate cyst counted. For calculation of the 95 % confidence intervals of the relative abundances the equation of Maher (1971) was used. Accumulation rates of dinoflagellate cysts were calculated by multiplying the sedimentation rates (Berger et al., 2002b) with the cyst concentrations per ml, which was calculated based on the known number of *Lycopodium* spores added in the form of tablets.

For 21 samples the total organic carbon (TOC) contents has been determined by decarbonating a sediment aliquot of ~ 25 mg using 6 N hydrochloric acid before combustion at 1050 °C in a Heraeus CHN-O-rapid elemental analyzer (see Rommerskirchen et al., 2011). This data set is complemented by TOC shipboard data published in Wefer et al. (1998) and shown in Fig. 4.

CPD
11, 1913–1943, 2015

4 Results

A total of 36 dinoflagellate cyst taxa were identified whereof the *Brigantedinium* spp. group is the dominant one. In Figs. 2 and 3 the percentages and accumulation rates of the most abundant species are shown. In general, both relative and absolute trends show similarity for each species. The record has been visually divided into 5 zones.

Zone I runs from the start of the record at 9 to 7.8 Ma. This zone is mainly characterized by cysts of the *Batiacasphaera micropapillata* complex with values mostly around 20 % reaching a maximum of 50 %. *Impagidinium paradoxum* is well represented (generally over 10 %) especially in the beginning with a peak over 20 %. *Lingulodinium machaerophorum* is present in all samples of Zone I, with two exceptions, reaches values up to 20 % at around 8.5 Ma, and decreases afterwards to a minor representation in the assemblages (Fig. 2). Cysts of *Nematosphaeropsis labyrinthus* reach up to maxima of 15 %. *Impagidinium* sp. 2 (De Schepper and Head, 2009) cysts are also present and make up around 5 % of the assemblage and have a maximum of 20 % at around 8.3 Ma. *Selenopemphix quanta* is only marginally represented in Zone I. *Brigantedinium* spp. have generally low values (around 5 %) that rise at the end of Zone I to around 15 %. Almost completely lacking in this interval are *Operculodinium centrocarpum* cysts.

Zone II (7.8–6.2 Ma) is marked by a decline of cysts abundance of the *B. micropapillata* complex to less than 10 % (and less than 5 % around 7 Ma). Additionally the absolute values are decreasing from around 3000 cysts cm^{-2} ka^{-1} to less than 1000. Values for *Brigantedinium* spp. and *S. quanta* cysts (Fig. 3) are increased in this zone but show decreasing trends towards the end of the Zone II at 6.5 Ma. Also *H. tectata* decreases from around 20 % to marginal occurrence at 6.5 Ma. However, an increasing trend shows the representation of *B. hirsuta* from low values of less than 10 % to more than 30 %. As in Zone I, *L. machaerophorum* is mostly represented with less than 10 % but peaks at ∼ 7.5 Ma with 63 % of the assemblage. Again *O. centrocarpum* is lacking.

CPD
11, 1913–1943, 2015

Zone III (6.2–5.5 Ma) is characterized by *H. tectata* cysts dominating the samples until 5.8 Ma and reaching values between 40 and 50 %. Additionally, the *S. quanta* curve increases again until 5 Ma. *Spiniferites* spp. and *B. hirsuta* values are also increasing between 6 and 5 Ma.

Zone IV (5.5–4.4 Ma) is characterized by *B. hirsuta* and *Brigantedinium* spp. *Brigantedinium* has low relative abundances until 5.2 but reaches 40 % later in Zone IV. Not represented is *L. machaerophorum*. The *B. micropapillata* complex is better represented in the period from 5.2 until 4.2 Ma with maxima around 25 % (Fig. 2). At around 4.8 Ma *Impagidinium* sp. 2 is well represented and peaks twice with values between 20 and 30 %.

Zone V (4.4–2.7 Ma) is defined by the representation of *O. centrocarpum* which is rising from a few percent at the start of the interval to 60 % at around 3.8 Ma. Towards the end *Brigantedinium* spp. and *Spiniferites* spp. cysts are increasing at the costs of *O. centrocarpum*.

In Fig. 4 the accumulation rates of summed dinoflagellate cysts are plotted against age. The accumulation rates of cysts range between 7000 and 93 000 cysts cm^{-2} ka^{-1}. One period with lower accumulation rates occurred until 8 Ma and two periods with generally higher accumulation rates were found between 8 and 6.4 Ma and from 5.4 to 4.2 Ma.

5 Discussion

5.1 Dinoflagellates as proxies for environmental conditions

Off the 2377 modern motile species listed worldwide (Gómez, 2012) only between 10 and 20 % of them produce cysts during their lifecycle that preserve well in the sediments (Head, 1996). The organic-walled cysts found in recent sediments around the world show a distribution that can be related to sea-surface gradients in temperature, salinity, nutrients and sea-ice cover (e.g. De Vernal et al., 1997; Dale et al., 2002;

Marret and Zonneveld, 2003; Holzwarth et al., 2007; Zonneveld et al., 2001, 2013). Therefore, it has been possible to use them as a tool to reconstruct surface waters conditions, e.g. nutrients and temperature, enabling past upwelling intensity variations. The dissolution of cysts sensitive to oxidative degradation (Zonneveld et al., 2001) such as *Brigantedinium* cannot entirely be dismissed but the relative high abundance of sensitive cysts throughout the record, as well as the high total concentration values (Fig. 4) suggest a minor effect. Therefore, we are confident to use the heterotrophic vs. autotrophic ratio (H/A ratio). The H/A ratio indicates upwelling (Lewis et al., 1990) based on the fact that the autotrophic dinoflagellates are in strong competition to diatoms whereas the heterotrophic ones feed on diatoms. Hence, high H/A ratio values reflect higher production. In our record the ratio is in good concordance to the total dinoflagellate cyst accumulation. Our results indicate five successive regimes (discussed below); a weak upwelling regime with strong influence of the warm waters of the Angola Current (Zone I, 9–7.8 Ma), an increase of upwelling linked to the intensification of the meridional temperature gradient in combination with Mio- to Pliocene uplift of south-western Africa (Zone II, 7.8–6.2 Ma), a period with exceptional conditions of increasing TOC and warmer SST (Zone III, 6.2–5.5 Ma) during the early stages of the Messinian Salinity Crisis (5.96–5.33 Ma), a resumption of productivity and upwelling after the Messinian (Zone IV, 5.5–4.4 Ma) and further intensification of the upwelling together with the effect of the Cunene River discharge (Zone V, 4.4–2.7 Ma).

5.2 The Angola–Benguela Front

ODP Site 1081 is located close to the modern position of the ABF, which offers opportunities to record changes in its position since the Miocene. The composition of the dinoflagellate cyst assemblages shows affinity to upwelling conditions over the entire record through nutrient indicating cyst species such as *Brigantedinium* spp., *S. quanta*, *L. machaerophorum* which is in accordance to an onset of the BUS before 10 Ma (e.g., Siesser, 1980; Diester-Haass et al., 1990; Heinrich et al., 2011; Rommerskirchen et al., 2011). However, fluctuations in accumulation rates and relative abundances, such as

CPD
11, 1913–1943, 2015

the presence or absence of *L. machaerophorum* and *O. centrocarpum*, indicate significant variability in the upwelling during the studied period. Open oceanic species, *Impagidinium paradoxum* (Dale et al., 2002; Zonneveld et al., 2013) and probably *Impagidinium* sp. 2 are stronger represented in Zones I and II (9–6.2 Ma) indicating warmer and less nutrient-rich environments. Before 7.8 Ma the *B. micropapillata* complex is well represented. Although the ecological background of the *B. micropapillata* complex is uncertain, studies from Zegarra and Helenes (2011) suggest this complex to be an indicator for warm nutrient-poor waters because it is often recorded together with other warm-water indicators. Hence, we consider *B. micropapillata* as an indicator of relative warm nutrient-poor conditions. The dinoflagellate cyst record corroborates the SST reconstruction of around 26 to 27 °C for Zone I (Hoetzel et al., 2013). During the early part of the record upwelling conditions were rather weak, which is also indicated by low TOC values (Fig. 4) (Wefer et al., 1998) and the influence of warm waters from the AC was still strong compared to later periods.

Southward penetration of the AC is also suggested by the presence of *L. machaerophorum* which today is not present in the BUS but in the area of the AC (Holzwarth et al., 2007). *L. machaerophorum* is an indicator for stratified warm nutrient-rich waters, e.g. after upwelling relaxation (Marret and Zonneveld, 2003; Zonneveld et al., 2013, and references therein) suggesting that periods with stratified water conditions were more frequent and/or longer than today. *I. paradoxum* and *N. labyrinthus* which are more frequent in waters around the ABF (Dale et al., 2002; Zonneveld et al., 2013) also may indicate a southern position of the ABF at least 3° of latitude further south than today. At present, the ABF shifts southwards on inter-annual timescales during Benguela Niños (Shannon et al., 1986). Under these special conditions, the waters over the Walvis Ridge receive a contribution of the Angola Current (Petterson and Stramma, 1991; Florenchie et al., 2004; Mohrholz et al., 2004; Richter et al., 2010). It is possible that these Benguela Niño events were more common during Miocene times when the SAA and the trade winds were weaker.

CPD
11, 1913–1943, 2015

5.3 Late Miocene upwelling intensification

Between 7.8 and 6.2 Ma (Zone II) dinoflagellate cyst accumulation rates are generally higher indicating higher productivity as the result of stronger upwelling (Fig. 4). Further support of the intensified upwelling is given by increased heterotrophic dinoflagellate cyst occurrences, such as *Selenopemphix* and *Brigantedinium* (Zonneveld et al., 2001), which is also shown in the increased H/A ratio (Fig. 4). Slightly higher TOC values as compared to the earlier period (Zone I; Fig. 4) underline increased upwelling conditions. In general, a gradual intensification of the BUS is suggested by other authors, e.g. Rommerskirchen et al. (2011) who showed for ODP Site 1085 a strong sea-surface cooling until 6 Ma. Early during the interval (prior to 7 Ma) periods of weaker upwelling and stronger influence of warmer waters may have occurred over the Walvis Ridge allowing the presence and even the dominance at 7.5 Ma of *L. machaerophorum*. However, while it is likely that the ABF was weaker and located further to the south and that the influence of the AC was stronger due to more frequently occurring Benguela Niño conditions, its influence seems to disappear towards the end of Zone II, after 7 Ma. This is indicated by the low occurrences of *L. machaerophorum* and the increase in relative cyst abundance of oceanic species such as *I. paradoxum* and the *B. micropapillata* complex. Our data record a northward shift and intensification of the ABF implying a restriction of the AC to latitudes north of 19° S as well as open ocean conditions over the site. This interpretation is corroborated by the SST record (Hoetzel et al., 2013) showing a cooling trend between 7.8 and 6.2 Ma and by the TOC record showing reduced values towards the end of the period between 6.7 and 6.5 Ma (Fig. 4).

5.4 Exceptional conditions during the Mediterranean Salinity Crisis

Zone III (6.2–5.5 Ma) coincides mostly with the Messinian Salinity Crisis (5.96–5.33 Ma; Krijgsman et al., 1999). Mediterranean deepwater formation was weakened since 7.2 Ma (Kouwenhoven and Van der Zwaan, 2006) although a connection between the Atlantic Ocean and the Mediterranean Sea remained until the later halite phase be-

CPD
11, 1913–1943, 2015

tween 5.61 and 5.55 Ma (Topper and Meijer, 2013). The Mediterranean begun to desiccate shortly before 6.2 Ma, creating salty and dense waters flowing into the Atlantic and contributing to NADW formation until 6.0 Ma (Pérez-Asensio et al., 2012). Further restriction of the Mediterranean Outflow Water between 6.0 and 5.5 Ma weakened the AMOC, although the effects of the Mediterranean Outflow Water on the AMOC strongly depend on the salinity of the Outflow Water (Ivanovic et al., 2014). An earlier salinity crisis in the Mediterranean occurred during the Tortonian between 7.8 and 7.6 Ma (Kouwenhoven et al., 2003).

Between 6.2 and 5.8 Ma the record shows dominance of *H. tectata* which is known to be a cool-water tolerant species mostly of the Pliocene and Pleistocene of the North Atlantic region (Head, 1994; Louwye et al., 2004; Versteegh, 1997) but also of the Miocene (Head et al., 1989; Jimenez-Moreno et al., 2006). This maximum of *H. tectata* is flanked by two maxima in the occurrence of *B. hirsuta* (6.8–6.4 and 5.6–5.2 Ma) and an earlier max of *H. tectata* occurred between 7.8 and 7.6 Ma. Both, *H. tectata* and *B. hirsuta* have not yet been described from the BUS area but they alternatively dominate the assemblages from 6.8 to 5.2 Ma, representing unique conditions which did not exist before or after that period.

De Schepper et al. (2011) showed that *H. tectata* exceeded 30 % of the dinoflagellate cyst assemblages when the reconstructed Mg/Ca sea-surface temperatures were between 10 and 15 °C. Although *H. tectata* has not yet been described from the South Atlantic, it probably represents strong surface water cooling. However, SST estimates of ODP Site 1081 only show a moderate cooling (Hoetzel et al., 2013). According to Vidal et al. (2002), the sedimentation rates at ODP Site 1085 increased between 6.1 and 5.8 Ma which they correlate to the occurrences of strong glacial events. *S. quanta* is also increased during that period, indicating a higher nutrient supply suggesting increased upwelling. On the other hand, other heterotrophic taxa (e.g. *Brigantedinium* spp.) have low values and consequently the H/A ratio is lower than before although some upwelling is suggested by relative high TOC (Fig. 4).

CPD
11, 1913–1943, 2015

For the period from 6.5–5.0 Ma, Rommerskirchen et al. (2011) described TEX86 temperature estimates from ODP Site 1085 indicating warming of subsurface waters around 6.3 Ma and between 5.6 and 5.2 Ma. They concluded that the subsurface water warming resulted from a downward mixing of heat caused by a weakening of the AMOC and reduced NADW formation related to reduced outflow of salty Mediterranean water. The period of warm subsurface waters at Site 1085 coincides with the increased representations of *B. hirsuta* suggesting that the downward mixing affected the quality of upwelled waters at the ODP Site 1081 creating special and non-recurring conditions.

Berger et al. (2002a) argued that the quality of the coastal upwelling waters at the BUS is linked to the deep water circulation and the strength of the NADW. Increasing NADW formation brings, until a critical point, more silica from the Northern Ocean into the Southern Ocean and eventually changes the chemistry of the upwelled waters at the BUS (enabling the Matuyama Diatom Maximum). Changes of the silica content might have affected dinoflagellates indirectly via ecological competition with algae or other microorganisms or via changes in food supply and sources. The latter one is important for the heterotrophic species since they feed on diatoms which are highly depending on silica contents.

A further change of the quality of the upwelled waters could be caused by a poleward undercurrent flowing south from the Angola dome along the African margin transporting silica-rich, phosphate-rich and oxygen depleted waters (Berger et al., 1998) and increasing the fertile thermocline. A strengthening of this undercurrent and a higher silica content of the waters representing a mixing of the intermediate water and this poleward undercurrent is indicated by a radiolarian peak from 5.8 until 5.25 Ma at ODP Site 1085 (Diester-Haass et al., 2002) coinciding with the younger *B. hirsuta* maximum. The peak in radiolarian might explain lower H/A ratios since radiolarian might have competed with heterotrophic dinoflagellates.

CPD
11, 1913–1943, 2015

5.5 Resumption of upwelling

Around 5.6 Ma at ODP Site 1081 (Zone IV) and between 5.6 and 5.3 Ma at Site 1085 (Rommerskirchen et al., 2011), maxima in SST estimates are recorded after which SSTs fluctuated around a cooling trend during the rest of the Pliocene. Resumption of upwelling in the BUS area is also indicated by a sharp increase of *Brigantedinium* spp. around 5.3 Ma corresponding to increased sedimentation rates at ODP Site 1085 (Diester-Haass et al., 2002). Additionally, high H/A ratios and increasing TOC indicate increased primary production at Site 1081 (Fig. 4). After 5.33 Ma, the Gibraltar strait opened and again very salty and dense Mediterranean Outflow Water could re-intensify NADW formation and AMOC (Ivanovic et al., 2014). More important for the intensification of the BUS Upwelling however, might have been the uplift of south-western Africa during the Pliocene (Partridge, 1997; Roberts and White, 2010). Uplift would have strengthened the coastal low-level winds and increased Ekman pumping causing enhanced upwelling (Jung et al., 2014).

5.6 Upwelling intensification and river supply

The presence and dominance of *O. centrocarpum* since 4.4 Ma (Zone V) indicate nutrient-rich and well mixed waters representing conditions adjacent to strong upwelling and/or river outflow (Dale et al., 2002). Although *O. centrocarpum* is a cosmopolitan species, it occurs in the South East Atlantic in vicinity to the upwelling area (Dale et al., 2002; Marret and Zonneveld, 2003; Holzwarth et al., 2007; Zonneveld et al., 2013). It is, additionally, represented in turbulent and well mixed waters at the boundary of coastal and oceanic waters (Wall et al., 1977; Dale et al., 2002). *L. machaerophorum* is, however, completely absent, indicating that the partly warm stratified conditions of the Miocene have been completely replaced by stronger upwelling, better mixing, and cooler conditions. The increase of *Brigantedinium* spp. abundance and the high TOC concentration (between 4 and 5 WT%; Fig. 4) and further decreasing SSTs (Hoetzel et al., 2013) underline nutrient rich conditions of a strong upwelling.

Between 4.4 and 3.0 Ma, the H/A ratios show minima during dinoflagellate cyst flux maxima indicating again a change in the quality of upwelled waters corresponding to a northward shift of diatom assemblages to the central BUS area (Marlow et al., 2000). These changes can be linked to a stronger influence of Antarctic Intermediate Water.

The increase of *Spiniferites* at the end of the record might be linked to more coastal conditions and river input (Dale et al., 2002). Increased river discharge could also explain relative high occurrences of *O. centrocarpum*. The desiccation and outflow of the Cunene lake through the Cunene river is supposed to have started in the early Pliocene (Hipondoka, 2005).

5.7 Links to oceanic and global climate change

The intensification of the BUS and the steepening of the ABF imply strengthening of SE trade winds and the regional wind maximum (Benguela Jet) along the coast (Nicholson, 2010). It should be kept in mind that the period under discussion concerns the early stages of upwelling of the northern BUS and that upwelling further intensified during the Pleistocene (Berger et al., 2002a, b); in this region SSTs dropped by 10 °C during the past 2.5 Ma (Rosell-Melé et al., 2014).

Prior to 8 Ma, sub-Antarctic stable oxygen isotope values indicate slightly warmer temperatures and less intense glaciations in Antarctica (Billups, 2002). The polar front was probably weaker and situated more southwards and so was the SAA. Additionally, glaciations in the Northern Hemisphere were not yet extensive so that the meteorological equator might have been located further north than today creating a weak meridional temperature and pressure gradient in the Southern Hemisphere (Flohn, 1981). A weak meridional temperature gradient would shift the ABF southwards and allow the AC to penetrate southwards over the Walvis Ridge creating Benguela Niño like conditions (sensu Shannon et al., 1986). Conversely, increase of the meridional gradient (Billups, 2002) would have resulted in a northward shift of the ABF, northward migration of the BUS (Diester-Haass et al., 1992), stronger currents and vigorous trade winds. Additionally, Mio- to Pliocene uplift of Southern Africa intensified the near-

CPD
11, 1913–1943, 2015

coastal low-level Benguela Jet and consequently increased upwelling of the BUS (Jung et al., 2014).

The strengthened winds in turn, especially the stronger Benguela Jet, led to aridification of the south-western coast of Africa since warm and humid air from the Atlantic would be hindered to reach large areas of Namibia. Moreover, a stronger Benguela Jet led to intensified upwelling and lower SSTs, which would also act to reduce rainfall. Dupont et al. (2013) discuss, based on pollen data and deuterium values of plant waxes from ODP Site 1085, that the aridification is caused by a decrease of precipitation derived from the Atlantic and that the main source area of precipitation changed to the Indian Ocean, as is the case today (Gimeno et al., 2010). Mio- to Pliocene mountain uplift would have helped to both strengthen the Benguela Jet as well as to block South Atlantic air from reaching far into the continent (Jung et al., 2014). The expansion of the grass savanna between 8 and 3 Ma and subsequent expansion of the desert, is linked to this aridification (Hoetzel et al., 2013).

The period from 6.8 until 5.2 Ma when the representations of *H. tectata* and *B. hirsuta* dominate forms an interlude in the development of upwelling. It is a period of global oceanic and climate changes contemporaneously to the initiation of the NADW formation (Billups, 2002), the desiccation of the Mediterranean Sea (Krijgsman et al., 1999) and the loss of contact between the deep waters of the Pacific and Atlantic Oceans by the decreasing sill depth of the CAS. Changes in the AMOC and the NADW formation would have resulted in changes of the subsurface waters and thus in the quality of upwelled waters (Berger et al., 2002a), which resulted in a unique flora of the BUS.

From 4.4 Ma on, final closure of the CAS and the emergence of the Panama Isthmus (Steph et al., 2010) proceeded, leading to the intensification of the AMOC and deep water formation (Haug and Tiedemann, 1998) changing the intermediate waters of the BUS which again changed the dinoflagellate assemblages. Since 3.2 Ma the intensification of the Northern Hemisphere glaciations and the introduction to a bi-polar icehouse started the Inter-Tropical Convergence Zone shifted southwards to its average modern position (Billups et al., 1999). The southward shift probably caused an

CPD
11, 1913–1943, 2015

intensified meridional temperature gradient and a further intensification of the low-level winds driving upwelling, which is recorded by the dinoflagellate cyst assemblages.

6 Summary and conclusions

A record of organic-walled dinoflagellate cysts in association with total organic carbon data was used to reconstruct changes in upwelling conditions over the Walvis Ridge from the Late Miocene to the early Pliocene near its northern boundary, the Angola Benguela Front. Here we report about the early stages of upwelling. A weak pressure system and an ABF located further south resulted in more frequently occurring Benguela Niño-conditions, which effects were recorded for the period prior to 7.8 Ma. The meridional temperature gradient steepened afterwards inducing a northward migration of the ABF. The Benguela Niño-conditions were especially manifested by the occurrence of *L. machaerophorum*, a species blooming in warm stratified nutrient-rich waters after upwelling relaxation. The intensification of the upwelling is shown by decreases of warm water indicating taxa and increases in indicators of cold and nutrient-rich conditions. Production was high until around 7 Ma and the portion of heterotrophic species was enhanced.

Between 6.8 and 5.2 Ma, *B. hirsuta* and *H. tectata* were abundant during a period with exceptional oceanic conditions related to the Messinian Salinity Crisis. *B. hirsuta* occurred during times with relaxed North Atlantic Deepwater production and reduced Atlantic overturning circulation whereas *H. tectata* occurred during a time of increased NADW production directly before the desiccation of the Mediterranean Basin. The shoaling of the Central American Seaway and later the intensification of the Northern Hemisphere glaciations enhanced NADW production changing the quality of upwelled waters. Miocene to Pliocene uplift of Southern Africa further increased upwelling of the Benguela Upwelling System. Remote influence of fresh water after the start of Cunene River discharge into the South Atlantic is indicated by the first occurrence of *O. centrocarpum*.

CPD
11, 1913–1943, 2015

Acknowledgements. This work was supported by the DFG Research Center/Cluster of Excellence "MARUM – The Ocean in the Earth System" and "GLOMAR – Bremen International Graduate School for Marine Sciences". The authors thank Michael Schreck and Jens Matthiesen for helping to identify unknown dinoflagellates. Florian Rommerskirchen is thanked for the biogeochemical measurements and Marta Witek for laboratory support. Data can be found at Pangaea.de.

The article processing charges for this open-access publication were covered by the University of Bremen.

References

Berger, W. H., Wefer, G., Richter, C., Lange, C. B., Giraudeau, J., Hermelin, O., and Shipboard Scientific Party: The Angola–Benguela Upwelling System: paleoceanographic synthesis of shipboard results from leg 175, in: Proceedings of the Ocean Drilling Program, Initial Reports, 175, Ocean Drilling Program, College Station TX, USA, 505–531, 1998.

Berger, W. H., Lange, C. B., and Pérez, M. E.: The early Matuyama Diatom Maximum off SW Africa: a conceptual model, Mar. Geol., 180, 105–116, 2002a.

Berger, W. H., Lange, C. B., and Wefer, G.: Upwelling history of the Benguela-Namibia System: a synthesis of leg 175, Results, in: Proceedings of the Ocean Drilling Program, Scientific Results, 175, Ocean Drilling Program, College Station TX, USA, 1–103, 2002b.

Billups, K.: Late Miocene through early Pliocene deep water circulation and climate change viewed from the sub-Antarctic South Atlantic, Palaeogeogr. Palaeocl., 185, 287–307, 2002.

Billups, K. and Schrag, D. P.: Paleotemperatures and ice volume of the past 27 Myr revisited with paired Mg/Ca and $^{18}O/^{16}O$ measurements on benthic foraminifera, Paleoceanography, 17, 1003, doi:10.1029/2000PA000567, 2002.

Billups, K., Ravelo, A. C., Zachos, J. C., and Norris, R. D.: Link between oceanic heat transport, thermohaline circulation, and the Intertropical Convergence Zone in the early Pliocene Atlantic, Geology, 27, 319–322, 1999.

Butzin, M., Lohmann, G., and Bickert, T.: Miocene ocean circulation inferred from marine carbon cycle modeling combined with benthic isotope records, Paleoceanography, 26, PA1203, doi:10.1029/2009PA001901, 2011.

Dale, B., Dale, A. L., and Jansen, J. H. F.: Dinoflagellate cysts as environmental indicators in surface sediments from the Congo deep-sea fan and adjacent regions, Palaeogeogr. Palaeocl., 185, 309–338, 2002.

De Schepper, S. and Head, M. J.: Age calibration of dinoflagellate cyst and acritarch events in the Pliocene–Pleistocene of the eastern North Atlantic (DSDP Hole 610A), Stratigraphy, 5, 137–161, 2008.

De Schepper, S. and Head, M. J.: Pliocene and Pleistocene dinoflagellate cyst and acritarch zonation of DSDP Hole 610A, Eastern North Atlantic, Palynology, 33, 179–218, 2009.

De Schepper, S., Fischer, E. I., Groeneveld, J., Head, M. J., and Matthiessen, J.: Deciphering the palaeoecology of Late Pliocene and Early Pleistocene dinoflagellate cysts, Palaeogeogr. Palaeocl., 309, 17–32, 2011.

De Vernal, A., Rochon, A., Turon, J.-L., and Matthiessen, J.: Organic-walled dinoflagellate cysts: palynological tracers of sea-surface conditions in middle to high latitude marine environments, Geobios, 30, 905–920, 1997.

De Verteuil, L. and Norris, G.: Miocene protoperidiniacean dinoflagellate cysts from the Maryland and Virginia coastal plain, in: Neogene and Quaternary Dinoflagellate Cysts and Acritarchs, American Association of Stratigraphic Palynologists Foundation, Dallas TX, USA, 391–430, 1992.

Diester-Haass, L.: Sea level changes, carbonate dissolution and history of the Benguela Current in the Oligocene–Miocene off Southwest Africa (DSDP Site 362, Leg 40), Mar. Geol., 79, 213–242, 1988.

Diester-Haass, L., Meyers, P. A., and Rothe, P.: Miocene history of the Benguela Current and Antarctic ice volumes: evidence from rhythmic sedimentation and current growth across the Walvis Ridge (Deep Sea Drilling project sites 362 and 532), Paleoceanography, 5, 685–707, 1990.

Diester-Haass, L., Meyers, P. A., and Rothe, P.: The Benguela Current and associated upwelling on the southwest African margin: a synthesis of the Neogene–Quaternary sedimentary record at DSDP sites 362 and 532, Geol. Soc. London, Spec. Publ., 64, 331–342, 1992.

Diester-Haass, L., Meyers, P. A., and Vidal, L.: The late Miocene onset of high productivity in the Benguela Current upwelling system as part of a global pattern, Mar. Geol., 180, 87–103, 2002.

CPD

11, 1913–1943, 2015

Miocene–Pliocene stepwise intensification of the Benguela upwelling

S. Hoetzel et al.

Dupont, L. M., Rommerskirchen, F., Mollenhauer, G., and Schefuß, E.: Miocene to Pliocene changes in South African hydrology and vegetation in relation to the expansion of C_4 plants, Earth Planet. Sc. Lett., 375, 408–417, 2013.

Etourneau, J., Ehlert, C., Frank, M., Martinez, P., and Schneider, R.: Contribution of changes in opal productivity and nutrient distribution in the coastal upwelling systems to Late Pliocene/Early Pleistocene climate cooling, Clim. Past, 8, 1435–1445, doi:10.5194/cp-8-1435-2012, 2012.

Flohn, H.: A hemispheric circulation asymmetry during Late Tertiar, Geol. Rundsch., 70, 725–736, 2012, 1981.

Florenchie, P., Reason, C. J. C., Lutjeharms, J. R. E., Rouault, M., Roy, C., and Masson, S.: Evolution of interannual warm and cold events in the Southeast Atlantic Ocean, J. Climate, 17, 2318–2334, 2004.

Flower, B. P. and Kennett, J. P.: The middle Miocence climatic transition: east Antarctic ice sheet development, deep ocean circulation and global carbon cycling, Palaeogeogr. Palaeocl., 108, 537–555, 1994.

Gimeno, L., Drumond, A., Nieto, R., Trigo, R. M., and Stohl, A.: On the origin of continental precipitation, Geophys. Res. Lett., 37, 1–7, 2010.

Goldner, A., Huber, M., and Caballero, R.: Does Antarctic glaciation cool the world?, Clim. Past, 9, 173–189, doi:10.5194/cp-9-173-2013, 2013.

Gómez, F.: A checklist and classification of living Dinoflagellates (Dinoflagellata, Alveolata), CICIMAR Oceánides, 27, 65–140, 2012.

Haug, G. H. and Tiedemann, R.: Effect of the formation of the Isthmus of Panama on Atlantic Ocean thermohaline circulation, Nature, 393, 673–676, 1998.

Head, M. J.: Morphology and paleoenvironmnental significance of the Cenozoic dinoflagellate genera *Tectatodinium* and *Habibacysta*, Micropaleontology, 40, 289–321, 1994.

Head, M. J.: Modern dinoflagellate cysts and their biological affinities, in: Palynology: Principles and Applications, American Association of Stratigraphic Palynologists Foundation, Salt Lake City UT, USA, 1197–1248, 1996.

Head, M. J., Norris, G., and Mudie, P. J.: Palynology and dinocyst stratigraphy of the Miocene in ODP leg 105, hole 645E, Baffin Bay, in: Proceeding Ocean Drilling Program, Scientific Results, 105, Ocean Drilling Program, College Station TX, USA, 467–514, 1989.

Heinrich, S., Zonneveld, K. A. F., Bickert, T., and Willems, H.: The Benguela upwelling related to the Miocene cooling events and the development of the Antarctic Circumpolar

Current: evidence from calcareous dinoflagellate cysts, Paleoceanography, 26, PA3209, doi:10.1029/2010PA002065, 2011.
Hipondoka, M.: The Development and Evolution of Etosha Pan, Namibia, Ph.D. thesis, Julius-Maximilian-Universität Würzburg, Germany, 152 pp., 2005.
Hirst, A. C. and Hastenrath, S.: Atmosphere–Ocean Mechanisms of climate anomalies in the Angola–Tropical Atlantic sector, J. Phys. Oceanogr., 13, 1146–1157, 1983.
Hoetzel, S., Dupont, L., Schefuß, E., Rommerskirchen, F., and Wefer, G.: The role of fire in Miocene to Pliocene C_4 grassland and ecosystem evolution, Nat. Geosci., 6, 1027–1030, 2013.
Holzwarth, U., Esper, O., and Zonneveld, K.: Distribution of organic-walled dinoflagellate cysts in shelf surface sediments of the Benguela upwelling system in relationship to environmental conditions, Mar. Micropaleontol., 64, 91–119, 2007.
Ivanovic, R. F., Valdes, P. J., Flecker, R., and Gutjahr, M.: Modelling global-scale climate impacts of the late Miocene Messinian Salinity Crisis, Clim. Past, 10, 607–622, doi:10.5194/cp-10-607-2014, 2014.
Jimenez-Moreno, G., Head, M. J., and Harzhauser, M.: Early and Middle Miocene dinoflagellate cyst stratigraphy of the Central Paratethys, Central Europe, J. Micropalaeontol., 25, 113–139, 2006.
Jung, G., Prange, M., and Schulz, M.: Uplift of Africa as a potential cause for Neogene intensification of the Benguela Upwelling System, Nat. Geosci., 7, 741–747, 2014.
Knorr, G. and Lohmann, G.: Climate warming during Antarctic ice sheet expansion at the Middle Miocene transition, Nat. Geosci., 7, 376–381, 2014.
Kostianoy, A. G. and Lutjeharms, J. R. E.: Atmospheric effects in the Angola–Benguela Frontal Zone, J. Geophys. Res., 104, 20963–20970, 1999.
Kouwenhoven, T. H., Hilgen, F. J., and Van der Zwaan, G. J.: Late Tortonian–early Messinian stepwise disruption of the Mediterranean–Atlantic connections: constraints from benthic foraminiferal and geochemical data, Palaeogeogr. Palaeocl., 198, 303–319, 2003.
Kouwenhoven, T. J. and Van der Zwaan, G. J.: A reconstruction of late Miocene Mediterranean circulation patterns using benthic foraminifera, Palaeogeogr. Palaeocl., 238, 373–385, 2006.
Krijgsman, W., Hilgen, F. J., Raffi, I., Sierro, F. J., and Wilson, D. S.: Chronology, causes and progression of the Messinian salinity crisis, Nature, 400, 652–655, 1999.
Lewis, J., Dodge, J. D., and Powell, A. J.: Quaternary dinoflagellate cysts from the upwelling system offshore Peru, Hole 686B, ODP Leg 112, in: Proceedings of the Ocean Drilling Pro-

CPD
11, 1913–1943, 2015

Miocene–Pliocene stepwise intensification of the Benguela upwelling

S. Hoetzel et al.

gram, Scientific Results, 112, Ocean Drilling Program, College Station TX, USA, 323–328, 1990.
Louwye, S., Head, M. J., and De Schepper, S.: Dinoflagellate cyst stratigraphy and palaeoecology of the Pliocene in northern Belgium, southern North Sea Basin, Geol. Mag., 141, 353–378, 2004.
Lutjeharms, J. R. E. and Meeuwis, J. M.: The extent and variability of South-East Atlantic upwelling, S. Afr. J. Marine Sci., 5, 51–62, 1987.
Lutjeharms, J. R. E. and Stockton, P. L.: Kinematics of the upwelling front off southern Africa, S. Afr. J. Marine Sci., 5, 35–49, 1987.
Maher, L. J. J.: Nomograms for computing 0.95 confidence limits of pollen data, Rev. Palaeobot. Palynol., 13, 85–93, 1971.
Marlow, J. R., Lange, C. B., Wefer, G., and Rosell-Mele, A.: Upwelling intensification as part of the Pliocene–Pleistocene climate transition, Science, 290, 2288–2291, 2000.
Marret, F. and Zonneveld, K. A. F.: Atlas of modern organic-walled dinoflagellate cyst distribution, Rev. Palaeobot. Palyno., 125, 1–200, 2003.
Meeuwis, J. M. and Lutjeharms, J. R. E.: Surface thermal characteristics of the Angola–Benguela Front, S. Afr. J. Marine Sci., 9, 261–279, 1990.
Mohrholz, V., Schmidt, M., Lutjeharms, J. R. E., and John, H.-C.: Space–time behaviour of the Angola–Benguela Frontal Zone during the Benguela Niño of April 1999, Int. J. Remote Sens., 25, 1337–1340, 2004.
Nicholson, S. E.: A low-level jet along the Benguela coast, an integral part of the Benguela current ecosystem, Climate Change, 99, 613–624, 2010.
Nicholson, S. E. and Entekhabi, D.: Rainfall variabillity in equatorial and southern Africa: relationships with sea surface temperatures along the southwestern coast of Africa, J. Clim. Appl. Meteorol., 26, 561–578, 1987.
Partridge, T.: Cainozoic environmental change in southern Africa, with special emphasis on the last 200 000 years, Prog. Phys. Geog., 21, 3–22, 1997.
Pérez-Asensio, J. N., Aguirre, J., Schmiedl, G., and Civis, J.: Impact of restriction of the Atlantic–Mediterranean gateway on the Mediterranean outflow water and eastern Atlantic circulation during the Messinian, Paleoceanography, 27, PA3222, doi:10.1029/2012PA002309, 2012.
Petterson, R. G. and Stramma, L.: Upper-level circulation in the South Atlantic Ocean, Prog. Oceanogr., 26, 1–73, 1991.

CPD
11, 1913–1943, 2015
Miocene–Pliocene stepwise intensification of the Benguela upwelling
S. Hoetzel et al.

Poore, H. R., Samworth, R., White, N. J., Jones, S. M., and McCave, I. N.: Neogene overflow of northern component water at the Greenland–Scotland Ridge, Geochem. Geophy. Geosy., 7, Q06010, doi:10.1029/2005GC001085, 2006.

Richter, I., Behera, S. K., Masumoto, Y., Taguchi, B., Komori, N., and Yamagata, T.: On the triggering of Benguela Niños: remote equatorial versus local influences, Geophys. Res. Lett., 37, L20604, doi:10.1029/2010GL044461, 2010.

Roberts, G. G. and White, N.: Estimating uplift rate histories from river profiles using African exsamples, J. Geophys. Res., 115, B02406, doi:10.1029/2009JB006692, 2010.

Rommerskirchen, F., Condon, T., Mollenhauer, G., Dupont, L., and Schefuß, E.: Miocene to Pliocene development of surface and subsurface temperatures in the Benguela Current System, Paleoceanography, 26, PA3216, doi:10.1029/2010PA002074, 2011.

Rosell-Melé, A., Martínez-Garciac, A., and McClymont, E. L.: Persistent warmth across the Benguela upwelling system during the Pliocene epoch, Earth Planet. Sc. Lett., 386, 10–20, 2014.

Rouault, M.: South east tropical Atlantic warm events and southern African rainfall, Geophys. Res. Lett., 30, 8009, doi:10.1029/2002GL014840, 2003.

Schreck, M., Matthiessen, J., and Head, M. J.: A magnetostratigraphic calibration of Middle Miocene through Pliocene dinoflagellate cyst and acritarch events in the Iceland Sea (Ocean Drilling Program Hole 907A), Rev. Palaeobot. Palyno., 187, 66–94, 2012.

Shannon, L. V., Boyd, A. J., Brundrit, G. B., and Taunton-Clark, J.: On the existence of an El Niño-type phenomenon in the Benguela System, J. Mar. Res., 44, 495–520, 1986.

Siesser, W. G.: Late Miocene origin of the Benguela Upwelling System off northern Namibia, Science, 208, 283–285, 1980.

Steph, S., Tiedemann, R., Prange, M., Groeneveld, J., Schulz, M., Timmermann, A., Nürnberg, D., Rühlemann, C., Saukel, C., and Haug, G. H.: Early Pliocene increase in thermohaline overturning: a precondition for the development of the modern equatorial Pacific cold tongue, Paleoceanography, 25, PA2202, doi:10.1029/2008PA001645, 2010.

Summerhayes, C. P., Kroon, D., Rosell-Melé, A., Jordan, R. W., Schrader, H.-J., Hearn, R., Villanueva, J., Grimalt, J. O., and Eglinton, G.: Variability in the Benguela Current upwelling system over the past, Prog. Oceanogr., 35, 207–251, 1995.

Topper, R. P. M. and Meijer, P. T.: A modeling perspective on spatial and temporal variations in Messinian evaporite deposits, Mar. Geol., 336, 44–60, 2013.

CPD
11, 1913–1943, 2015

Miocene–Pliocene stepwise intensification of the Benguela upwelling

S. Hoetzel et al.

Udeze, C. and Obohikuenobe, F.: Neogene palaeoceanographic and palaeoclimatic events inferred from palynological data: Cape Basin off South Africa, ODP Leg 175, Palaeogeogr. Palaeocl., 219, 199–223, 2005.
Versteegh, G. J. M.: The onset of major Northern Hemisphere glaciations and their impact on dinoflagellate cysts and acritarchs from the Singa section, Calabria (southern Italy) and DSDP Holes 607/607A (North Atlantic), Mar. Micropaleontol., 30, 319–343, 1997.
Vidal, L., Bickert, T., Wefer, G., and Röhl, U.: Late Miocene stable isotope stratigraphy of SE Atlantic ODP Site 1085: relation to Messinian events, Mar. Geol., 180, 71–85, 2002.
Wall, D., Dale, B., Lohmann, G. P., and Smith, W. K.: The environmental and climatic distribution of dinofalgellate cysts in modern marine sediments from regions in the North and South Atlantic Oceans and adjacent seas, Mar. Micropaleontol., 2, 121–200, 1977.
Wefer, G., Berger, W. H., Richter, C., Adams, D. D., Anderson, L. D., Andreasen, D. J., Brüchert, V., Cambray, H., Christensen, B. A., Frost, G. M., Giraudeau, J., Gorgas, T. J., Hermelin, J. O. R., Jansen, J. H. F., Lange, C. B., Laser, B., Lin, H.-L., Maslin, M., Meyers, P. A., Motoyama, I., Murray, R. W., Perez, M. E., Pufahl, P. K., Spiess, V., Vidal, L., Wigley, R., and Yamazaki, T.: Site 1081, in: Proceedings Ocean Drilling Program, Initial Reports, 175, Ocean Drilling Program, College Station TX, USA, 223–727, 1998.
Wright, D., Miller, G., and Fairbanks, G.: Early and Middle Miocene stable isotopes: implications for deepwater circulation and climate, Paleoceanography, 7, 357–389, 1992.
Zachos, J., Pagani, M., Sloan, L., Thomas, E., and Billups, K.: Trends, rhythms, and aberrations in global climate 65 Ma to present, Science, 292, 686–693, 2001.
Zegarra, M. and Helenes, J.: Changes in Miocene through Pleistocene dinoflagellates from the Eastern Equatorial Pacific (ODP Site 1039), in relation to primary productivity, Mar. Micropaleontol., 81, 107–121, 2011.
Zonneveld, K. A. F., Versteegh, G. J. M., and De Lange, G. J.: Palaeoproductivity and post-depositional aerobic organic matter decay reflected by dinoflagellate cyst assemblages of the Eastern Mediterranean S1 sapropel, Mar. Geol., 172, 181–195, 2001.
Zonneveld, K. A. F., Marret, F., Versteegh, G. J. M., Bogus, K., Bonnet, S., Bouimetarhan, I., Crouch, E., de Vernal, A., Elshanawany, R., Edwards, L., Esper, O., Forke, S., Grøsfjeld, K., Henry, M., Holzwarth, U., Kielt, J.-F., Kim, S.-Y., Ladouceur, S., Ledu, D., Chen, L., Limoges, A., Londeix, L., Lu, S.-H., Mahmoud, M. S., Marino, G., Matsouka, K., Matthiessen, J., Mildenhal, D. C., Mudie, P., Neil, H. L., Pospelova, V., Qi, Y., Radi, T., Richerol, T., Rochon, A., Sangiorgi, F., Solignac, S., Turon, J.-L., Verleye, T., Wang, Y., Wang, Z., and Young, M.: Atlas

Discussion Paper | Discussion Paper | Discussion Paper | Discussion Paper |

of modern dinoflagellate cyst distribution based on 2405 datapoints, Rev. Palaeobot. Palyno., 191, 1–197, 2013.

CPD
11, 1913–1943, 2015

Miocene–Pliocene stepwise intensification of the Benguela upwelling

S. Hoetzel et al.

Table 1. Recognised species ordered after metabolism.

Autotrophic species	
Impagidinium	sp. 2 (De Schepper and Head, 2009)
	aculeatum
	paradoxum
	sphaericum
	patulum
	strialatum
Operculodinium	spp.
	centrocarpum
	israelianum
	janduchenei
Pentapharsodinium	*dalei*
Lingulodinium	*machaerophorum*
Spiniferites	spp.
	ramosus
	mirabilis
	cf. *mirabilis*
	membranaceus
Achomosphaera	spp.
Nematosphaeropsis	*labyrinthus*
Batiacasphaera	*micropapillata*
	hirsuta
Tuberculodinium	*vancampoae*
Pyxidinopsis	*reticulata*
Habibacysta	*tectata*
Ataxodinium	*zevenboomii*
	confusum
Heterotrophic species	
Brigantedinium	spp.
Selenopemphix	*quanta*
	nephroides
	brevispinosa
	brevispinosa conspica
	armageddonensis
Trinovantedinium	*glorianum*
	papulum
	fergnomatum
	applanatum
Lejeunecysta	spp.
	oliva
	sabrina
Quinquecuspis	*concreta*
Unknown, further species	
Sumatradinium	*soucouyanatae*

CPD
11, 1913–1943, 2015
Miocene–Pliocene stepwise intensification of the Benguela upwelling
S. Hoetzel et al.

Title Page
Abstract | Introduction
Conclusions | References
Tables | Figures
◀I | ▶I
◀ | ▶
Back | Close
Full Screen / Esc
Printer-friendly Version
Interactive Discussion

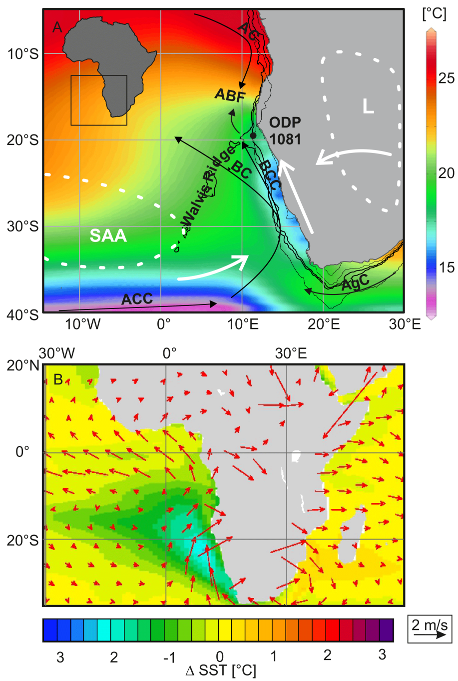

Figure 1. (a) Map with location of ODP Site 1081 within the South East Atlantic showing the mean annual temperatures in colours (Ocean Data View, U.S. NODC World Ocean Atlas 2009), oceanic features in black (AC: Angola Current, ABF: Angola–Benguela Front, BC: Benguela Current, BCC: Benguela Coastal Current, ACC: Antarctic Circumpolar Current, AgC: Agulhas Current) and main atmospheric features in white (SAA: South Atlantic Anticyclone, 1020 mbar; L(low): 1006 mbar). Mean atmospheric sea level pressure cells of January after (Petterson and Stramma, 1991). **(b)** Effect of uplift of Southern Africa on Benguela Upwelling. Changes in surface wind in m s^{-1} and sea surface temeprature (SST) in °C according to a CCSM3 model run configurated with full uplift minus one without (Jung et al., 2014).

CPD

11, 1913–1943, 2015

Title Page
Abstract | Introduction
Conclusions | References
Tables | Figures
◄| |►
◄ ►
Back | Close
Full Screen / Esc
Printer-friendly Version
Interactive Discussion

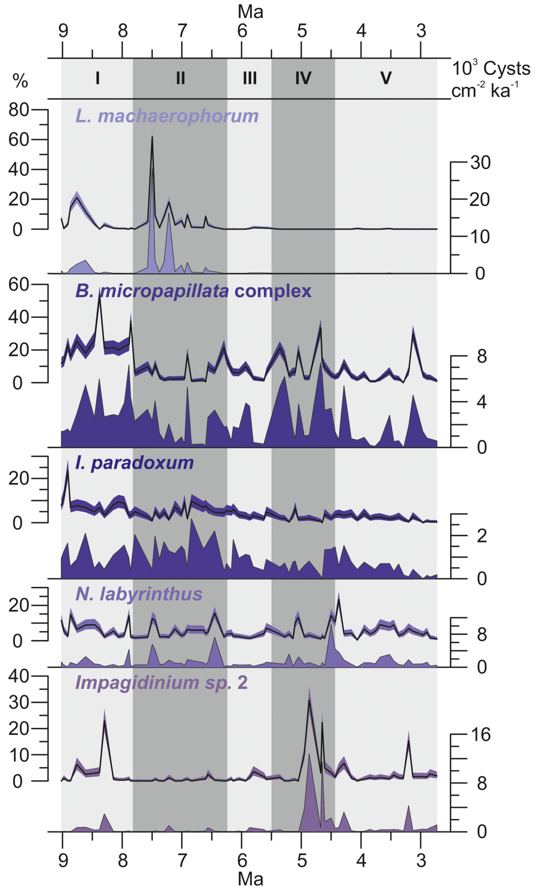

Figure 2. Relative and absolute abundances of selected dinoflagellate cysts within the zoning scheme (grey boxes) used in the text. The percentages are shown by lines (left Y axes), shadings represent 95 % confidence intervals. Accumulation rates are shown by the filled-in graphs (right Y axes).

CPD
11, 1913–1943, 2015

Title Page
Abstract | Introduction
Conclusions | References
Tables | Figures
◀I | ▶I
◀ | ▶
Back | Close
Full Screen / Esc
Printer-friendly Version
Interactive Discussion

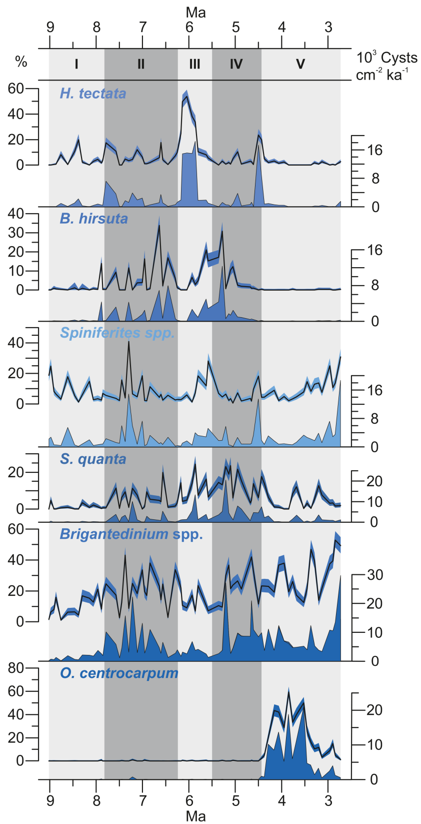

Figure 3. Relative and absolute abundances of selected dinoflagellate cysts within the zoning scheme (grey boxes) used in the text. The percentages (left *Y* axes) are shown by lines, shadings represent 95 % confidence intervals. Accumulation rates are shown by the filled-in graph (right *Y* axes).

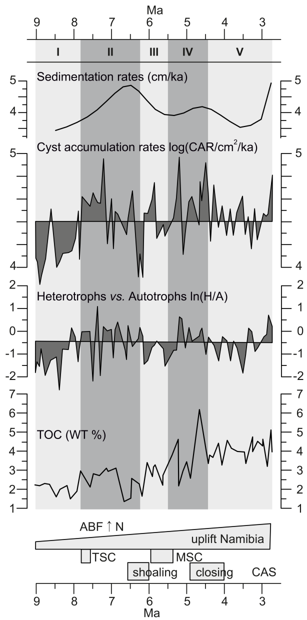

Figure 4. Sedimentation rates (after Berger et al., 2002b), total dinocyst accumulation rates (CAR $cm^2\,ka^{-1}$ on a log scale), ratio between heterotroph and autotroph dinoflagellate cysts (ln scale), total organic carbon (TOC in weight percentages after Wefer et al. (1998) complemented by unpublished data by Florian Rommerskirchen). Zoning follows Fig. 2. At the bottom timing of global events that would have influenced sea surface conditions in the Benguela region; shift of Angola Benguela Fron (ABF) northwards, increased uplift of Namibia since 30 Ma (Robets and White, 2010); timing of the Tortonian Salinity Crisis (TSC) and Messinian Salinity Crisis (MSC) in the Mediterranean (Kouwenhoven et al., 2003; Krijgsman et al., 1999); timing of the shoaling (Billups, 2002), respectively closing (Steph et al., 2010) of the Central American Seaway (CAS).

CPD
11, 1913–1943, 2015